

# High Frequency and High Luminance AC-PDP Sustaining Driver

Seong-Wook Choi\*, Sang-Kyoo Han\*\* and Gun-Woo Moon†

\*Dept. of Electrical Engineering and Computer Science, Korea Advanced Institute of Science and Technology, Korea

\*\*School of Electrical Engineering, Kookmin University, Korea

## ABSTRACT

Plasma display panels (PDPs) have a serious thermal problem, because the luminance efficiency of a conventional PDP is about 1.5 lm/W and it is less than 3~5 lm/W of a cathode ray tube (CRT). Thus there is a need for improving the luminance efficiency of the PDP. There are several approaches to improve the luminance efficiency of the PDP and we adopted a driving PDP at high frequency range from 400 kHz up to over 700 kHz. Since a PDP is regarded as an equivalent inherent capacitance, many types of sustaining drivers have been proposed and widely used to recover the energy stored in the PDP. However, these circuits have some drawbacks for driving PDPs at high frequency ranges. In this paper, we investigate the effect of the parasitic components on the PDP itself and on the driver when the reactive energy of the panel is recovered. Various drivers are classified and evaluated based on their suitability for high frequency drivers. Finally, a current-fed driver with a DC input voltage bias is proposed. This driver overcomes the effect of parasitic components in the panel and driver. It fully achieves a ZVS of all full-bridge switches and reduces the transition time of the panel polarity. It is tested to validate the high frequency sustaining driver and the experimental results are presented.

**Keywords:** plasma display panel (PDP), energy recovery, high frequency driver

## 1. Introduction

The recent interest in flat panel display devices, because PDPs have been praised for its large screen size, wide viewing angle, thinness, and high contrast, has made an alternating current (AC) PDP a promising candidate for conventional CRT display<sup>[1]</sup>. However, PDPs have a serious heat problem, because the energy conversion efficiency is very low as shown in Fig. 1. It is reported that the luminance efficiency of a PDP is 1.5 lm/W and it

is less than 3~5 lm/W of CRT. Thus, there is a need for improving the luminance efficiency of the AC-PDP.

There are several approaches to improve the luminance efficiency of PDPs. The first method is changing the cell structure to spread out more phosphor in the cells. The second method is increasing the Xenon ratio of the discharge gas mixture to obtain more ultraviolet rays (UV). Another method is driving the PDP at a higher frequency than usual<sup>[2]</sup>. The operation of the PDP can be divided into three periods: resetting, addressing and sustaining periods. Actually, most of the light emission occurs during the sustaining period. As mentioned above, high frequency driving means increasing the frequency of the sustaining pulse from conventional 200 kHz up to over 700 kHz. After consideration of these methods, we adopted the driving PDP at high frequency range to improve the

---

Manuscript received Sept. 15, 2005; revised Dec. 14, 2005

†Corresponding Author: gwmoon@ee.kaist.ac.kr

Tel: +82-42-869-3475, Fax: +82-42-861-3475, KAIST

\*Dept. of Electrical Engineering and Computer Science, KAIST

\*\*School of Electrical Engineering, Kookmin University

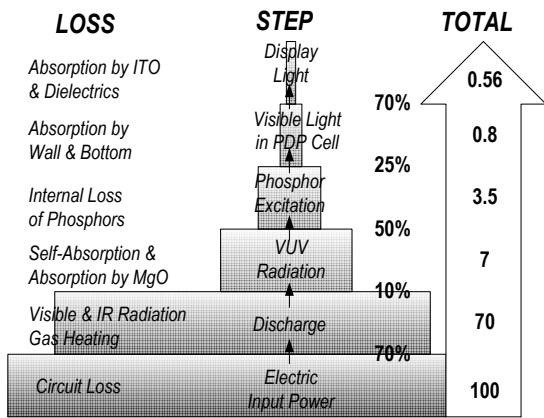


Fig. 1 Energy Conversion efficiency of AC-PDP

luminance efficiency.

However, there is a serious problem accompanied by increasing the frequency of the sustaining pulse. Since the sustaining electrodes of the PDP are covered with a dielectric and MgO layer, a PDP can be regarded as an equivalent inherent capacitance  $C_p$  as shown in Fig. 2. Therefore, considerable energy of  $2C_pV_s^2$  for each sustaining cycle is dissipated in the non-ideal resistance circuits and the PDP during charging or discharging intervals<sup>[3]</sup>. Also the sustaining driver, which has a well-known full-bridge configuration with four sustain switches, suffers from a large capacitive displacement current, which can give rise to electromagnetic interference noise (EMI). To relieve these problems, many types of sustaining drivers, which reduce the capacitive displacement current and heating problem of switching devices by adopting the LC resonant technique, have been proposed<sup>[3-12]</sup>. However, these circuits have serious drawbacks in driving the PDP at the high frequency.

In this paper, hitherto developed various energy recovery sustaining drivers are reviewed and compared to find the most suitable PDP driver for high frequency driving. First, we investigate the effect of the parasitic components of the PDP and driving circuit when the energy recovery function of the sustaining driver is performed. Secondly, various energy recovery sustaining drivers presented in [3]-[12] are classified according to voltage waveform across the PDP and current waveform through the energy recovery inductor. While each sustaining driver is evaluated for its suitability for the high

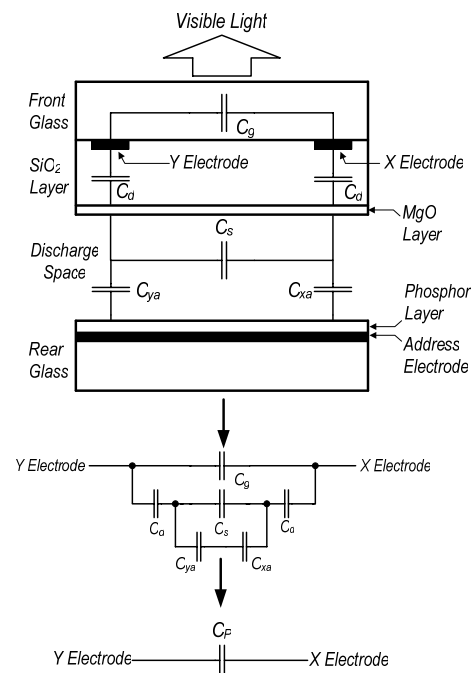


Fig. 2 Equivalent circuit of a three-electrode AC-PDP

frequency driver. Finally, considering all necessary aspects for the high frequency sustaining driver, the current-fed type with  $V_s$  bias is chosen as the best solution in this paper. This driver can overcome undesirable resonance among the parasitic components, ensures the zero voltage switching (ZVS) of all full-bridge inverter switches and reduces the transition time of the panel polarity, which is a very desirable merit for high frequency driving.

## 2. Effect of Parasitic Components

Fig. 3 shows the Weber energy recovery sustaining driver, which features high efficiency and good circuit

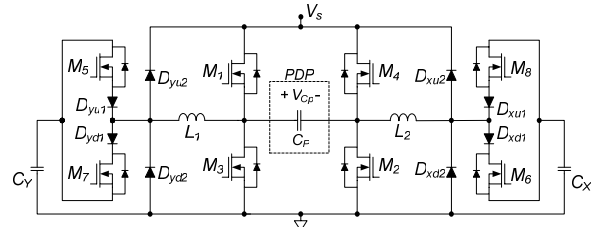


Fig. 3 Schematic diagrams of Weber energy recovery sustaining driver

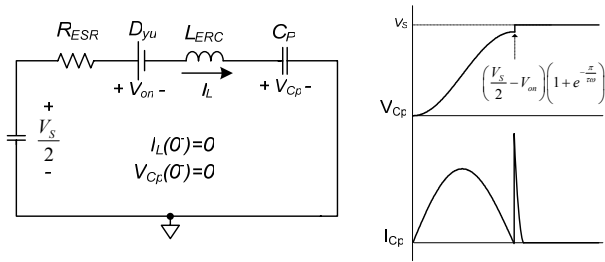


Fig. 4 Equivalent circuit and key waveforms of Weber driver considering parasitic resistance

flexibility to cope with various driving methods<sup>[4]</sup>. Although this driver is widely used in the digital display industry, it has several serious problems when operated at high frequency ranges. To explain the effect of the parasitic components, it is assumed that the Weber’s driver is operated at a high frequency range.

**2.1 Effect of parasitic resistance**

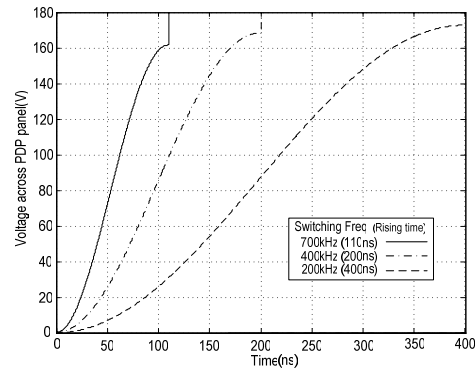
This driver has a severe problem in that the reactive energy stored in the PDP cannot be fully recovered and the ZVS operation of all power switches cannot be obtained under the existence of the parasitic resistance. Fig. 4 shows equivalent circuit and key waveforms with consideration of parasitic resistance during the energy recovery transient.

The current through panel  $I_{Cp}$  and the voltage across the PDP  $V_{Cp}$  are obtained as

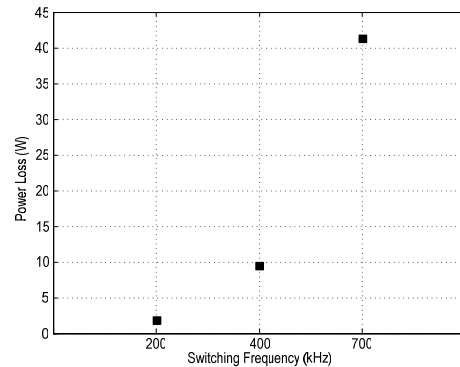
$$I_{Cp}(t) = \frac{1}{\omega L_{ERC}} \left( \frac{V_S}{2} - V_{on} \right) e^{-\frac{t}{\tau}} \sin(\omega t) \tag{1}$$

$$V_{Cp}(t) = \left( \frac{V_S}{2} - V_{on} \right) \left\{ 1 - e^{-\frac{t}{\tau}} \left( \cos(\omega t) + \frac{1}{\omega \tau} \sin(\omega t) \right) \right\} \tag{2}$$

where  $V_S$  = input sustaining voltage,  $\tau = 2L_{ERC} / R_{ESR}$ ,  $R_{ESR}$  = parasitic resistance of the driver,  $V_{ON}$  = forward voltage drop of the diode, and  $\omega = \sqrt{1 / \{L_{ERC}(2C_{OSS} + C_P)\} - 1 / \tau^2}$ . Fig. 5 shows the theoretical voltage waveforms and power losses as a function of the rising time of the sustaining pulse, according to the increasing frequency of the sustaining pulse. From these results, the sustaining driver suffers from heat problems due to the hard switching operation of



(a)



(b)

Fig. 5 Voltage waveforms and power losses caused by parasitic resistance according to increasing the frequency of sustaining pulse when ESR = 50mΩ is given: (a) Voltage waveforms across the PDP (b) Power losses

the sustain switches, which becomes more and more serious when increasing the frequency of the sustaining pulse.

**2.2 Effect of parasitic inductance**

It is very difficult to obtain the exact inductance for the energy recovery in practical implementation, because the required inductance at high frequency range is much smaller than the parasitic inductance of the driver board and connection cable between the PDP and driver. In this case especially, the energy current stored in the parasitic inductance is large enough to flow through the PDP in the opposite direction of the energy recovery current. This parasitic inductance disturbs the energy recovery action.

To figure out the parasitic inductance of the driver board and the PDP, the voltage waveforms across the

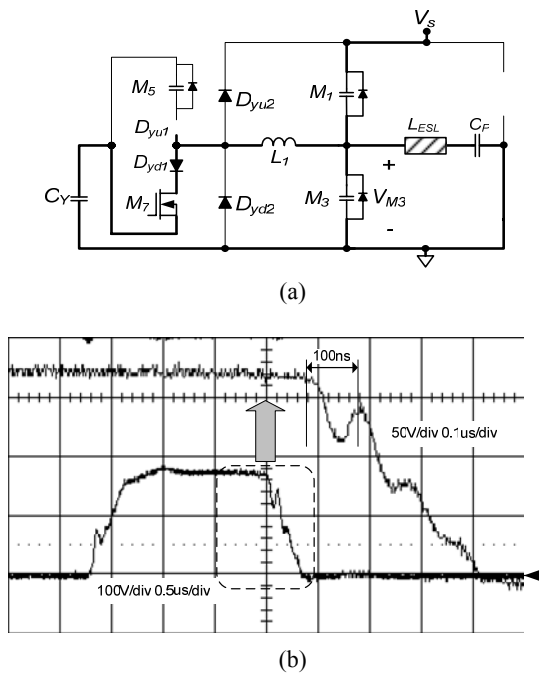


Fig. 6 Resonance due to parasitic inductance of driver and PDP in recovering the panel energy: (a) Schematic diagram of Weber driver in recovering the panel energy (b) Voltage waveforms across switch, M3

switch M<sub>3</sub> are measured at the operating frequency 200 kHz as shown in Fig. 6. As shown in Fig. 6b, the sub-oscillation is observed in the falling period of the sustaining pulse, which is because of the resonance between the parasitic inductance and output capacitance of the sustain switches. From this waveform, this parasitic inductance is roughly obtained as

$$L_{ESL} = \left( \frac{T_{osc}}{2\pi} \right)^2 \cdot \frac{1}{2 \times 2 \times C_{OSS}} \approx 63nH \quad (3)$$

where the switch output capacitor  $C_{OSS}=1nF$  is a known value and one resonant cycle of the sub-oscillation the measured value in Fig. 6b.

To explain the effect of the parasitic inductance in recovering the panel energy, a Weber driver operating at a switching frequency 700 kHz for a 42-in PDP ( $C_p=80nF$ ) is considered. If it is assumed that the rising/falling time of the panel voltage is 150ns, respectively and the switch output capacitor  $C_{OSS}$  given as 1nF, the energy recovery inductor can be determined as follows:

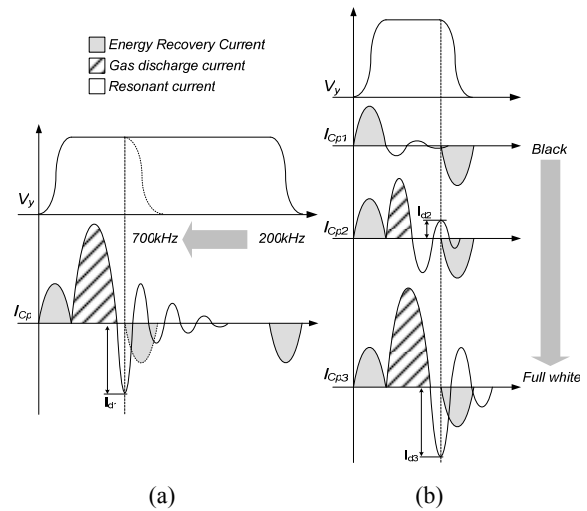


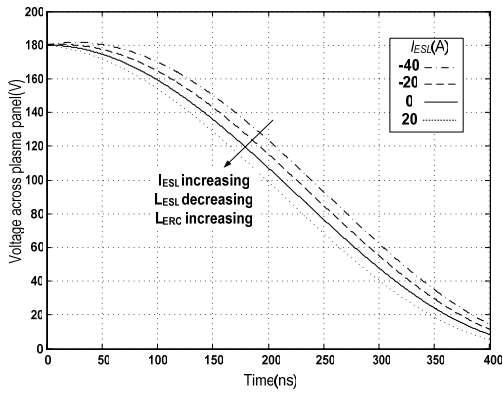
Fig. 7 Effect of resonance between parasitic inductance and panel capacitance: (a) when increasing frequency of sustaining pulse (b) when increasing amplitude of discharge current

$$L_{ERC} = \left( \frac{T_{rise}}{\pi} \right)^2 \cdot \frac{1}{C_p + 2 \times 2 \times C_{oss}} \approx 27nH \quad (4)$$

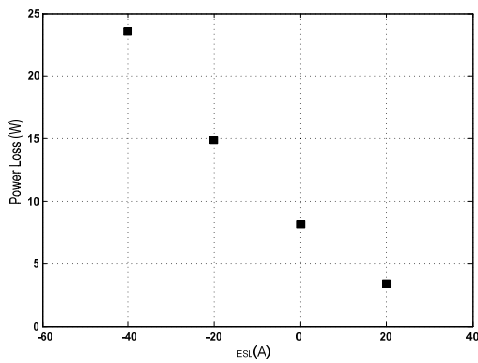
where  $T_{rise}$  is rising time of the panel voltage.

Equation (4) shows that the required energy recovery inductance (i.e.  $L_{ERC}=27nH$ ) is much smaller than the parasitic inductance (i.e.  $L_{ESL}=63nH$ ). These facts show that the complete energy recovery operation of the panel energy in a short period, such as 150nsec rising/falling time, is impossible under the existence of parasitic inductance. Moreover this parasitic inductance hinders the driver from energy recovery when the parasitic inductance has enough current energy to flow in the opposite direction of the energy recovery current. The parasitic inductance can have the initial value due to the following reasons.

The gas discharge current flows through the panel and the parasitic inductance. When the voltage across the panel reaches a breakdown point a visible light occurs. Then, the resonance between the panel capacitor and parasitic inductor of the driver and PDP begins immediately after the light emission comes to an end. At the next transition period of the panel polarity, the energy recovery operation at switching frequency 200 kHz is successfully performed. This is because the above



(a)



(b)

Fig. 8 Voltage waveforms across the PDP and power losses caused by the parasitic inductance when rising time = 400 ns and switching frequency = 700 kHz are given: (a) Voltage waveforms across PDP (b) Power losses

mentioned resonance is completely eliminated before the driver recovers the panel energy. However, when operating the Weber driver at a switching frequency over 200 kHz, the energy recovery function can not be guaranteed by the resonance as shown in Fig. 7a. Also, the amplitude of this resonant current is directly proportional to the amplitude of the discharge current or, in other words, the area of light emitted from the PDP as shown in Fig. 7b.

Fig. 8 shows the equivalent circuit and key waveforms of the Weber driver considering the parasitic inductance during the energy recovery transient. The current in panel,  $I_{Cp}$ , and the voltage across the panel are obtained as

$$I_{Cp}(t) = \frac{V_S/2 - V_{on}}{Z_O} \sin(\omega t) + \frac{L_{ESL}}{L_{ERC} + L_{ESL}} I_d \cos(\omega t) \quad (5)$$

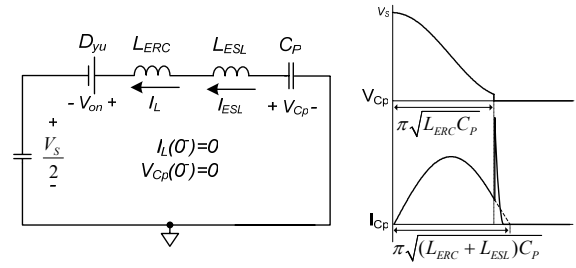


Fig. 9 Equivalent circuit and key waveforms of Weber driver considering parasitic inductance

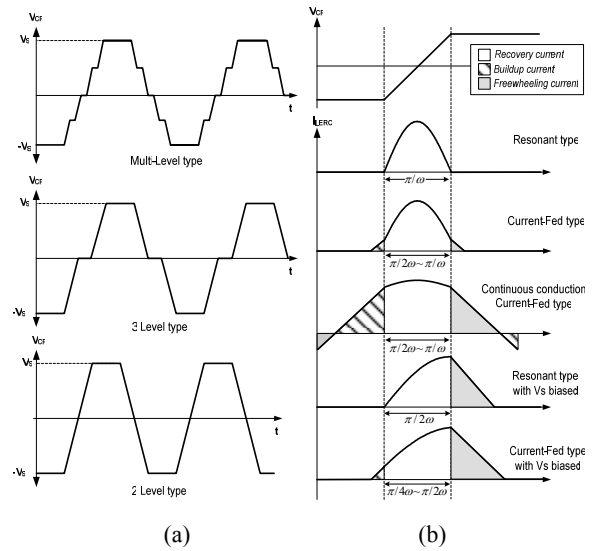


Fig. 10 Classification of energy recovery sustaining driver: (a) According to voltage waveform across PDP (b) Classifying Two-level type according to current waveform in energy recovery inductor

$$V_{Cp}(t) = V_S - \left( \frac{V_S}{2} - V_{on} \right) (1 - \cos(\omega t)) - \frac{I_d}{\omega C_P} \frac{L_{ESL}}{L_{ERC} + L_{ESL}} \sin(\omega t) \quad (6)$$

where  $I_d$  represents initial current through the parasitic inductance when the energy recovery function is achieved after the resonance between this inductance and inherent capacitance of panel,  $Z_O = \sqrt{(L_{ERC} + L_{ESL})/C_P}$ ,  $L_{ESL}$  = parasitic inductance of the driver and the PDP itself, and  $\omega = \sqrt{1/((L_{ERC} + L_{ESL})C_P)}$ .

Fig. 9 shows the theoretical waveforms and power losses according to the initial current of the parasitic inductance. Although there are no resistive components in equivalent circuit of the driver except for the reactive

components, the parasitic inductance and the energy stored in this inductance prevent the energy recovery function within the desired transition period. Especially, this problem is more serious when the direction of the initial current in this inductance goes against the current direction of the recovery inductor as shown in Fig. 9b.

### 3. Evaluation of Sustaining Drivers

As described in Section 2, the Weber sustaining driver widely used in commercial products is not suitable for high frequency drivers because of the parasitic resistance and inductance on the driver and the PDP itself. Therefore, to compensate the effect of the parasitic components, it is necessary to develop a high frequency sustaining driver with the ZVS operation.

The desired features of the high frequency sustaining driver can be summarized as follows.

a) The energy recovery function must be achieved within the transition time, below 200ns. This is essential to ensure a stable gas discharge and light waveform by making the effective pulse width, of the sustaining waveform, act as long as possible.

b) The sustaining driver has to simultaneously recover the reactive energy from both sides of the panel to reduce the transition time of the panel polarity.

c) The sustaining driver operated at high frequency should provide the PDP with more energy to compensate for power loss due to the parasitic resistance of driver and PDP itself. Since the power loss caused by an incomplete panel energy recovery is usually larger than the loss by the parasitic resistance, it is very important to ensure a complete energy recovery operation.

d) For effective energy recovery action, the sustaining driver must have larger energy recovery inductance than the parasitic one as stated in equation (6).

e) Even though the sustaining driver provides more energy to overcome the effect of the parasitic components, the power consumption in it should be minimized to improve the luminance efficiency of the AC-PDP.

The various sustaining drivers can be classified into three types according to the voltage waveform across the PDP and again, into five types according to the current waveform through the energy recovery inductor as shown

in Fig. 10. In view of the features mentioned above, each type of sustaining driver is evaluated for its suitability for a high frequency driver.

First, we consider the voltage waveform across the PDP to find out the proper sustaining driver at high frequency range. The multi-level types of sustaining drivers proposed in [5], [6] can not satisfy the required transition time because the energy recovery inductor of these drivers for desired rising and falling time must be much smaller than the parasitic inductance and it is very difficult to obtain an exact inductance of the energy recovery function in practical implementations. Also, the three-level types of sustaining drivers proposed in [4], [7], [8] are not suitable for high frequency drivers for the same reason that multi-level types of drivers are unsuitable. Since the two-level types of sustaining drivers proposed in [3] and [9-14] can change the polarity of the PDP at once, there is a possibility open to these drivers for high frequency driving.

Secondly, the two-level types of sustaining drivers are classified according to the shape of the current waveform in the energy recovery inductor as shown in Fig. 10b. Since the resonant two-level driver proposed in [10] can not fully recover the reactive energy of panel even with the absence of the parasitic inductance, this driver is not suitable for high frequency driver. Also, although the continuous conduction current-fed types of the two-level drivers proposed in [3], [9] have some desired features of the high frequency sustaining driver. These drivers can not be directly applied to a whole AC-PDP driver to display an image. Also they have a severe problem in that the energy recovery efficiency of this type is very low due to conduction loss of freewheeling current in the energy recovery inductor. The current-fed type drivers presented in [11], [12] have no bias voltage when the energy recovery function is achieved. Therefore, even though the energy recovery inductor of this driver has initial energy, this inductor is too small to guarantee a full recovery of the reactive energy of the panel at high frequency range.

The resonant type with a  $V_S$  bias<sup>[13]</sup> and a current-fed type with  $V_S$  bias<sup>[14]</sup> two-level sustaining driver can be adapted to a high frequency driver. However, the current-fed type with a  $V_S$  bias shows the best capability of recovering reactive energy from the panel during the

desired transition time regardless of the parasitic components of driver and the PDP itself. Fig. 11 shows the equivalent circuits of these sustaining drivers when reactive energy of the panel is recovered.

The voltages across the panel capacitance of each sustaining driver are obtained as

$$V_{Cp1}(t) = V_S(1 - 2\cos(\omega t)) - \frac{1}{\omega C_{P1}} \frac{L_{ESL}}{L + L_{ESL}} I_d \sin(\omega t) \quad (7)$$

$$V_{Cp2}(t) = V_S(1 - 2\cos(\omega t)) + \frac{1}{\omega C_P} \left( \frac{L I_i - L_{ESL} I_d}{L + L_{ESL}} \right) \sin(\omega t) \quad (8)$$

where  $V_{Cp1}$  = voltage across PDP of resonant type driver with  $V_S$  bias,  $V_{Cp2}$  = voltage across the PDP of a current-fed type driver with a  $V_S$  bias,  $L = L_{ERC1} + L_{ERC2}$ ,  $\omega = \sqrt{1/((L + L_{ESL})C_P)}$ .  $I_i$  represents the initial current in the energy recovery inductor to make this inductor act as a current source. As stated in (7) and (8), the initial current in the parasitic inductance,  $I_d$ , directly affects the operation of the resonant type driver with a  $V_S$  bias. While a current-fed type driver with a  $V_S$  bias ensures the energy recovery action even under the resonance of the parasitic component, since the initial current  $I_i$  in the energy recovery inductor compensates the initial current of the parasitic inductance. Therefore, this driver, current-fed with a  $V_S$  bias, overcomes the resonance of a parasitic component in panel and driver boards and fully achieves the ZVS of all full-bridge switches. In addition it reduces the transition time of the panel polarity, which is desirable for high frequency driving.

#### 4. Operation of High Frequency Driver

Fig. 12 shows the circuit diagram and its key waveforms of the chosen high frequency sustaining driver. For convenience of analysis, only the effect of parasitic inductor is considered, except for the parasitic resistor, because the energy recovery function of this driver can be fully achieved even under the existence of the parasitic resistance.

One cycle period of the chosen circuit is divided into two half cycles,  $t_0 \sim t_3$  and  $t_3 \sim t_6$ . As the operation principles of the two half cycles are symmetric, only the first half cycle is explained. Before  $t_0$ , the voltage  $V_{Cp}$  across  $C_P$  is

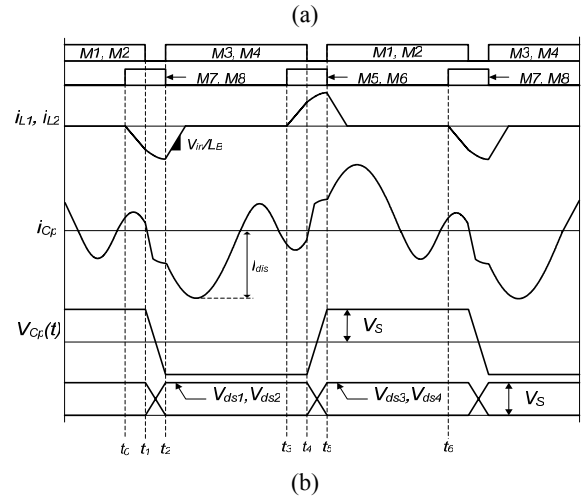
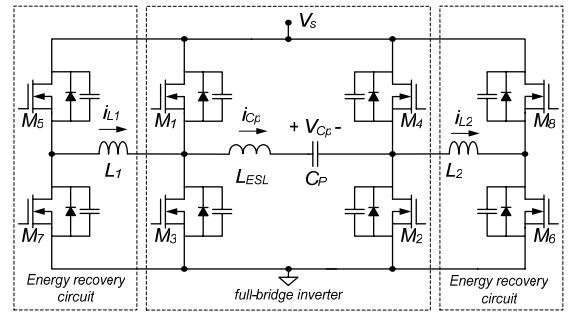


Fig. 11 Current-fed energy recovery sustaining driver with VS biased: (a) Schematic diagram (b) Key waveform

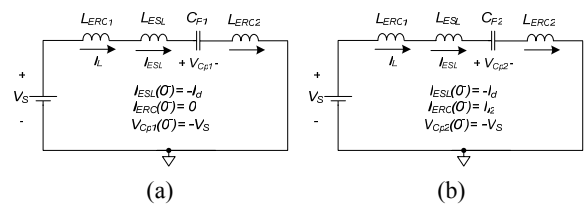


Fig. 12 Equivalent circuits of sustaining driver considering the resonance between parasitic inductance and panel capacitance: (a) resonant type with VS biased (b) current-fed type with VS biased

maintained at  $V_S$  with  $M_1$  and  $M_2$  conducting. Panel current,  $I_{Cp}$ , is in resonance due to parasitic inductance and panel capacitance.

**Mode 1 ( $t_0 \sim t_1$ )** : When  $M_7$  and  $M_8$  are turned on at  $t_0$ , Mode 1 begins. Input voltage  $V_S$  is applied to  $L_1$  and  $L_2$  with  $M_1, M_2, M_7,$  and  $M_8$  conducting. Thus,  $I_{L1}$  and  $I_{L2}$  increase linearly with the slope of  $V_S/L$  as  $I_{L1}(t) = I_{L2}(t) = V_S(t - t_0)/L$ , where it is assumed that the values of  $L_1$  and  $L_2$

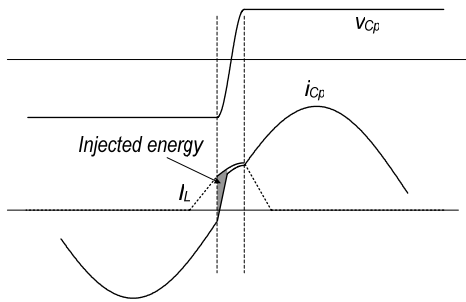


Fig. 13 Compensation of effect of panel resonance by current-fed type driver with VS biased

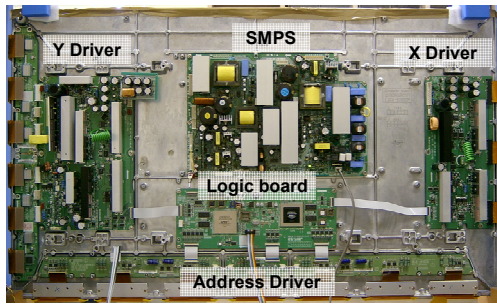


Fig. 14 42-in test PDP set for the proposed high frequency driver

are equal to  $L$ .  $I_{Cp}$  goes on with resonance.

**Mode 2** ( $t_1 \sim t_2$ ) : When  $M_1$  and  $M_2$  are turned off at  $t_1$ , Mode 2 begins. With the initial conditions of  $I_{L1}(t_1) = I_{L2}(t_1) = V_S (t_1 - t_0)/L$  and  $V_{Cp}(t) = V_S$ .  $I_{L1}$  and  $I_{L2}$  start to charge the PDP, but parasitic inductance disturbs this operation as follows:

$$I_{Cp}(t) = \frac{2V_S}{Z_o} \sin(\omega(t - t_1)) + \frac{LI_L(t_1) - L_{ESL}I_{Cp}(t_1)}{L + L_{ESL}} \cos(\omega(t - t_1)) \quad (9)$$

$$V_{Cp}(t) = V_S (1 - 2\cos(\omega(t - t_1))) + \frac{1}{\omega C_P} \left( \frac{LI_L(t_1) - L_{ESL}I_{Cp}(t_1)}{L + L_{ESL}} \right) \sin(\omega(t - t_1)) \quad (10)$$

where  $I_{Cp}$  = current through the PDP,  $V_{Cp}$  = voltage across the PDP of a current-fed type driver with  $V_S$  bias,  $L = L_1 + L_2$ ,  $\omega = \sqrt{1/((L + L_{ESL})C_P)}$ . Because this driver injects the PDP panel with an amount of energy proportional to  $(LI_L(t_1) - L_{ESL}I_{Cp}(t_1))$  regardless of the panel resonant current as shown in Fig. 13, the abrupt charging and discharging operations of  $C_P$  are avoided and the voltage across  $C_P$  is decreased towards  $-V_S$ .

**Mode 3** ( $t_2 \sim t_3$ ) : When  $V_{Cp}$  is clamped at  $-V_S$ , Mode 3

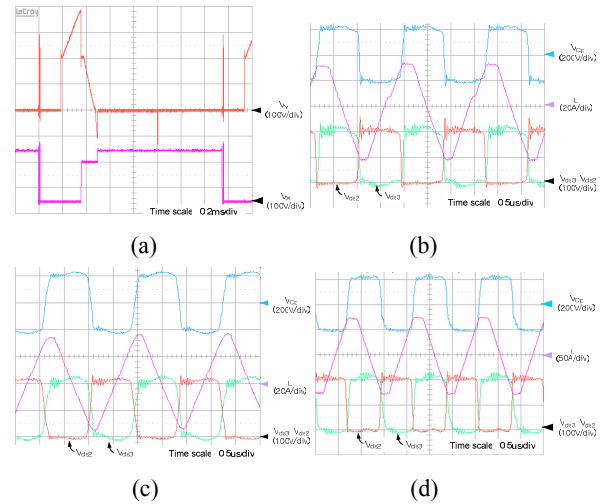


Fig. 15 Voltage and current waveforms of the proposed high frequency driver: (a) Voltage waveforms across panel during 1 subfield (b) sustaining waveform with 500kHz switching freq (c) sustaining waveform with 600kHz switching freq (d) sustaining waveform with 700kHz switching freq

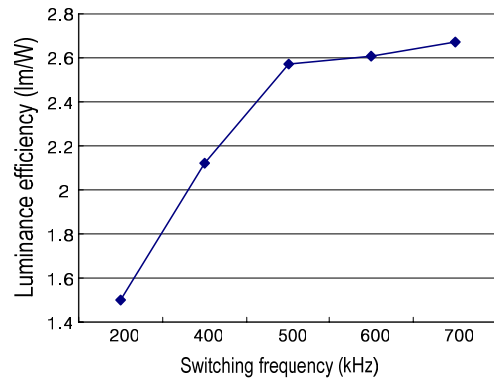


Fig. 16 Measured luminance efficiency of PDP

begins. Since voltage,  $V_{ds3}$  and  $V_{ds4}$ , across  $M_3$  and  $M_4$  are 0V,  $M_3$  and  $M_4$  can be turned on with the ZVS. After  $M_7$  and  $M_8$  are turned off, the currents in energy recovery inductor begin to decrease linearly with the slope of  $V_S/L$  and the energy stored in the inductors is fed back to the input power source. After the gas discharge current  $I_{dis}$  reaches 0A, resonance between the parasitic inductance and panel capacitance occurs. This resonance disturbs the energy recovery function of this driver in the next use.

The circuit operation of  $t_3 \sim t_6$  is similar to that of  $t_0 \sim t_3$ . Subsequently, the operation from  $t_0$  to  $t_6$  is repeated.



## 5. Experimental Results

To confirm the validity of the high frequency sustaining driver, a prototype PDP driver circuit was designed for a 42-in PDP with the following specifications:

- sustaining voltage:  $V_S = 200\sim 240$  V;
- switching frequency:  $f_S = 500\sim 700$  kHz;
- transition time:  $\Delta T = 200$ ns;
- panel capacitance:  $C_P =$  about 80 nF;
- scan method: single scan;
- test image pattern: full white.

The test set is as shown in Fig. 14. Fig. 15 shows the sustaining voltage and energy recovery inductor current waveforms of the high frequency sustaining driver. As can be seen in Fig. 15, the current source built in the inductor completely charges the panel capacitor  $C_P$  to  $V_S$  or  $-V_S$  regardless of the parasitic components. Fig. 16 shows that the measured luminance efficiency of the PDP is about 2.6 lm/W in a frequency range of 500 kHz to 700 kHz.

## 6. Conclusion

In this paper, we investigated the effect of the parasitic components of the PDP itself and the driver when energy recovery function of the sustaining driver is achieved. While various energy recovery sustaining drivers are examined to find an appropriate driver for operations at high frequency ranges. The drivers are classified and evaluated for its suitability for high frequencies. Also the desired features of high frequency drivers are suggested. With consideration of all the requirements for a high frequency driver, a current-fed type with a DC input voltage bias is proposed. This driver overcomes the effect of the parasitic components in the panel and driver. It fully achieves a zero voltage switching of all full-bridge switches and also reduces the transition time of the panel polarity. To validate the high frequency sustaining driver, it was tested on a 42-in panel. The experimental results are presented according to an increasing switching frequency of sustaining pulse in a range from 200 kHz to 700 kHz. With the proposed sustaining driver at 700 kHz switching frequency, the luminance efficiency is increased to about 2.6 lm/W.

## Acknowledgment

This work was supported by the Corporate R&D Center of Samsung SDI Corporation in Gyeonggi-Do, Republic of Korea.

## References

- [1] A. Sobel, "Plasma displays," *IEEE Trans. Plasma Sci.*, vol. 19, pp. 1032–1047, Dec. 1991.
- [2] J.H. Choi, et al. "Space charge effect for sustaining discharge in coplanar AC-PDP," *IDW'02*, pp873–876, 2002
- [3] S. Y. Lin, C. L. Chen, and K. M. Lee, "Novel regenerative sustain driver for plasma display panel," in *Proc. IEEE PESC'98*, pp 1739–1743, Fukuoka, Japan, 1998.
- [4] L. F. Weber and K. W. Warren, "Power efficient sustain drivers and address drivers for plasma panel," U.S. Patent 4 866 349, Sept. 1989.
- [5] C. W. Roh, H. J. Kim, S. H. Lee, and M. J. Youn, "Multilevel voltage wave-shaping display driver for AC plasma display panel application," *IEEE J. Solid-State Circ.*, Vol.38, No.6, pp.935–947, Jun. 2003.
- [6] C. W. Roh, "Novel plasma display driver with low voltage / current device stresses," *IEEE Trans. Con. Electron.*, Vol. 49, No. 4, pp.1360–1366, November 2003.
- [7] D. Y. Lee, J. H. Yang, and B. H. Cho, "Novel energy-recovery circuit for plasma display panel using regenerative transformer," in *Proc. IEEE PESC'03*, Vol.2, pp.656–659, June 2003.
- [8] H. van der Broeck, M. Wendt, "Alternative sustain driver concepts for plasma display panels," in *Proc. IEEE PESC'04*, Vol. 4, pp.2672–2677, June 2004.
- [9] S. K. Han, G. W. Moon, and M. J. Youn, "Current-fed energy-recovery circuit for plasma display panel," *Electronics Letters*, Vol. 39, Issue 14, pp 1035 – 1036, July 2003.
- [10] M. Ohba and Y. Sano, "Energy recovery driver for a dot matrix AC plasma panel with a parallel resonant circuit allowing power reduction," U.S. Patent 5 670 974, Sept. 1997.
- [11] C. C. Liu, H. B. Hsu, S. T. Lo, and C. L. Chen, "An energy-recovery sustaining driver with discharge current compensation for AC plasma display panel," *IEEE Trans. Ind. Electron.*, Vol. 48, No. 2, pp.344–351, Apr. 2001.
- [12] J. Y. Lee, J. S. Kim, N. S. Jung, and B. H. Cho, "The current injection method for AC plasma display panel (PDP) sustainer," *IEEE Trans. Ind. Electron.*, Vol. 51, No.

3, pp.615–624, Jun. 2004.

- [13] S. K. Han, G. W. Moon, and M. J. Youn, “A resonant energy-recovery circuit for plasma display panel employing gas-discharge current compensation method,” *IEEE Trans. Power Electron.*, Vol. 20, No.1 , pp. 209–217, Jan. 2005.
- [14] S. K. Han, G. W. Moon, and M. J. Youn, “A novel current-fed energy recovery sustaining driver for plasma display panel (PDP),” in *Proc. IEEE IECON '03*, Vol. 2 , pp. 1976–1980, Nov. 2003.



**Soeng-Wook Choi** received the B.S. degree in electrical engineering from Dankook University, Seoul, Korea, 2002, and the M.S. degree in electrical engineering from Korea Advanced Institute of Science and Technology (KAIST), Daejeon, in 2004, where he is currently pursuing the Ph.D. degree in electrical engineering. His research interests are in the areas of power electronics and digital display driver system, including analysis, modeling, design, and control of power converter, soft switching power converters, step-up power converters for electric drive system, multi-level converters and inverters, power factor correction, digital display driver systems, and EEFL back light inverters for LCD TV. Mr. Choi is a member of the Korean Institute of Power Electronics (KIPE).



**Sang-Kyoo Han** received the M.S. and Ph.D. degrees in Electrical Engineering and Computer Science from the Korea Advanced Institute of Science and Technology (KAIST), Daejeon, Korea, in 2001 and 2005, respectively. For six months after that, he worked as a post-doctoral fellow in KAIST where he developed digital display power circuits and performed several research activities. Since September 2005, he has been with the Kookmin University, Seoul, Korea, as a professor of electrical engineering and worked for the Samsung Power Electronics Center (SPEC) as a research fellow. His research interests are in the areas of power electronics and digital display driver system, including analysis, modeling, design, and control of power converter, soft switching power converters, step-up power converters for electric drive system, multi-level converters and inverters, power factor correction, Plasma Display Panel (PDP) driver, digital display driving circuit, and back light inverters for LCD TV. Mr. Han is a member of the Korean Institute of Power Electronics (KIPE).



**Gun-Woo Moon** was born in Korea in 1966. He received the B.S. degree from Han-Yang University, Seoul, Korea, and the M.S. and Ph.D. degrees in Electrical Engineering from the Korea Advanced Institute of Science and Technology (KAIST), Daejeon, in 1990, 1992, and 1996, respectively. He is currently an Associate Professor in the department of Electrical Engineering and Computer Science, KAIST. His research interests include modeling, design and control of power converters, soft-switching power converters, resonant inverters, distributed power systems, power-factor correction, electric drive systems, driver circuits of plasma display panels, and flexible ac transmission systems. Dr. Moon is a member of the Korean Institute of Power Electronics (KIPE), Korean Institute of Electrical Engineers (KIEE), Korea Institute of Telematics and Electronics (KITE), and Korea Institute of Illumination Electronics and Industrial Equipment (KIIIE).